Acta Crystallographica Section F
Structural Biology and Crystallization Communications
ISSN 1744-3091

Purification, crystallization and preliminary diffraction studies of an ectromelia virus glutaredoxin

John-Paul Bacik, Angela M. Brigley, Lisa D. Channon, Gerald F. Audette and Bart Hazes*

Department of Medical Microbiology and Immunology, 1-15 Medical Sciences Building, University of Alberta, Edmonton, Alberta T6G 2H7, Canada

Correspondence e-mail: bart.hazes@ualberta.ca

Received 2 March 2005
Accepted 26 April 2005
Online 1 June 2005

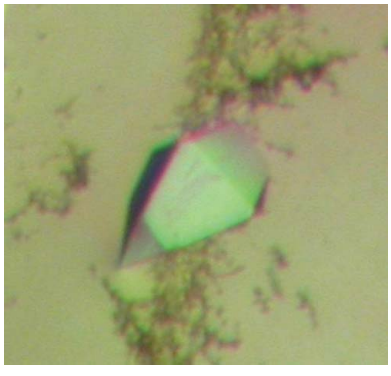

Ectromelia, vaccinia, smallpox and other closely related viruses of the orthopoxvirus genus encode a glutaredoxin gene that is not present in poxviruses outside of this genus. The vaccinia glutaredoxin O2L has been implicated as the reducing agent for ribonucleotide reductase and may thus play an important role in viral deoxyribonucleotide synthesis. As part of an effort to understand nucleotide metabolism by poxviruses, EVM053, the O2L ortholog of the ectromelia virus, has been crystallized. EVM053 crystallizes in space group $C222_1$, with unit-cell parameters a = 61.98, b = 67.57, c = 108.55 Å. Diffraction data have been processed to 1.8 Å resolution and a self-rotation function indicates that there are two molecules per asymmetric unit.

1. Introduction

Glutaredoxins form an important family of redox proteins that are found in prokaryotes and eukaryotes as well as viruses (reviewed in Fernandes & Holmgren, 2004). Their catalytic activity results from the alternate formation and reduction of a disulfide bond between a pair of cysteines in a characteristic C*XX*C sequence motif. The glutaredoxins resemble the thioredoxins and both families adopt a glutaredoxin/thioredoxin fold consisting of a four- to five-stranded mixed β-sheet flanked by three or four α-helices. The active-site cysteines of these proteins are located in a loop connecting the N-terminal β-strand to an α-helix. Thioredoxins are reduced directly by an NADPH-dependent thioredoxin reductase. For glutaredoxins, an NADPH-dependent glutathione reductase first produces reduced glutathione (GSH), which then reduces the glutaredoxin. While both glutaredoxins and thioredoxins reduce a variety of protein disulfides, glutaredoxins also have the unique ability to catalyse the formation and reduction of cysteine-GSH mixed disulfides (glutathionylation), which is used as a regulatory mechanism based on cellular redox potential (Gravina & Mieyal, 1993; Chai *et al.*, 2003).

The first glutaredoxin was discovered as a reducing agent for ribonucleotide reductase (RNR) in *Escherichia coli* (Holmgren, 1976). The actual target for reduction is a disulfide near the C-terminus of the large R1 subunit of the RNR–protein complex (Berardi *et al.*, 1998). Since RNR is the only enzyme that can reduce ribonucleotides to deoxyribonucleotides, it is absolutely required for DNA replication. Accordingly, RNR is found in all cellular organisms and mammalian RNR also uses a glutaredoxin as its reducing agent (Luthman *et al.*, 1979). Interestingly, all orthopoxviruses encode a glutaredoxin gene that is not present in viruses outside the orthopox genus and sequence analysis shows that this glutaredoxin is most closely related to the mammalian glutaredoxin involved in RNR reduction (results not shown). A role in ribonucleotide reduction is also consistent with the observation that all orthopoxviruses encode a viral RNR-R1 homolog, while RNR-R1 homologs are absent in all other poxviruses with the exception of swinepox. Furthermore, vaccinia virus lacking this glutaredoxin, known as O2L, has the same aberrant ribonucleotide-reduction phenotype as a virus lacking the RNR-R1 subunit (Rajagopal *et al.*, 1995).

With the knowledge that poxviral genome replication occurs outside of the nucleus and independent of the cell cycle, we are interested in the mechanisms of poxviral nucleotide metabolism. Given the likely role of O2L in deoxyribonucleotide production, we

have crystallized EVM053, the O2L ortholog from ectromelia virus strain Moscow (mousepox). Here, we report on the protein production, crystallization and diffraction data collection of EVM053 (12.3 kDa for the native protein) in the presence of the reducing agent DTT (5 m*M*). EVM053 shares 45% sequence identity with the human glutaredoxin Grx-1 for which an NMR structure is known (PDB code 1jhb; Sun *et al.*, 1998) and 43% identity with oxidized pig liver thioltransferase (PLTT) for which a 2.2 Å resolution crystal structure has been reported (PDB code 1kte; Katti *et al.*, 1995). These structures will be used as molecular-replacement search models for structure solution and for the analysis of the structural and functional consequences of the sequence variation in the viral enzyme.

2. Methods and results

2.1. Cloning, expression and purification

EVM053 was cloned into a pET-Blue2-based plasmid using a locally developed procedure (Hazes & Channon, unpublished results). The expression construct encodes an N-terminal His_6-tag sequence (MHHHHHH) followed by the entire EVM053 open reading frame. Arabinose-inducible BL-21 AI cells were used as the expression host strain. Protein expression from recombinant BL-21 AI cells was started by a 1:100 dilution of overnight culture into 2 l Erlenmeyer flasks containing 500 ml Luria–Bertani (LB) broth with 50 µg ml^{-1} carbenicillin. Cells were cultured at 310 K with shaking until an absorbance of A_{600} = 0.5–0.8 was reached. Protein expression was induced by adding arabinose to 0.05% followed by an incubation period of 3 h at 310 K. Cultures were centrifuged at 4000*g* for 20 min and the cell pellets were resuspended in 10 ml column buffer (10 m*M* Tris pH 8.0, 500 m*M* sodium chloride). The resuspended cells were sonicated and cell debris removed by centrifugation at 9000*g* for 30 min at 277 K. The supernatant was passed through a 0.45 µm filter prior to purification by liquid chromatography.

As the first purification step, the filtered supernatant was loaded onto an Ni^{2+}-charged HiTrap affinity column equilibrated with column buffer on an Akta Purifier (GE Healthcare) at 277 K. The column was washed with ten column volumes of wash buffer (10 m*M* Tris pH 8.0, 20 m*M* sodium chloride, 5 m*M* imidazole), after which the protein was eluted with a linear gradient of wash and elution buffers (10 m*M* Tris pH 8.0, 20 m*M* sodium chloride, 200 m*M* imidazole) over 20 column volumes. By eluting the protein in a low ionic strength buffer, the peak fraction could be loaded directly onto an anion-exchange chromatography column filled with Resource 30Q resin (GE Healthcare), which was pre-equilibrated with loading buffer (20 m*M* sodium chloride, 10 m*M* Tris pH 8.0). After washing the column with three column volumes of loading buffer, the protein was eluted with a linear gradient of loading buffer and elution buffer (250 m*M* sodium chloride, 10 m*M* Tris pH 8.0). SDS–PAGE analysis of the purified recombinant EVM053 product revealed a single band at the expected molecular weight of 13.3 kDa. A 5K NMWL membrane centrifugal filter device (Millipore) was used to exchange the buffer to 100 m*M* sodium chloride, 10 m*M* Tris pH 8.0 and to concentrate the sample. Protein concentration was assessed by BCA assay and amino-acid composition analysis prior to crystallization trials.

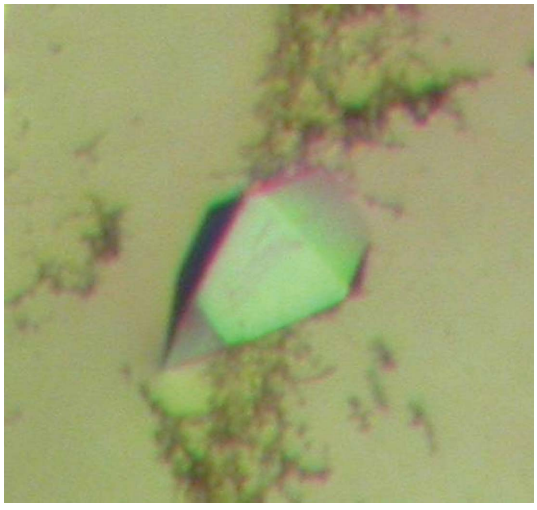

Figure 1
A typical crystal of EVM053. Dimensions are 0.30 × 0.20 × 0.075 mm.

Table 1
Summary of data-collection statistics.

Values in parentheses are for the highest resolution shell.

Resolution (Å)	36.20–1.80 (1.90–1.80)
No. of observations	113946 (6928)
No. of unique reflections	20896 (2737)
Completeness (%)	96.7 (88.0)
R_{sym}	0.135 (0.655)
$\langle I/\sigma(I)\rangle$	10.6 (1.8)
B_{Wilson} (Å^2)	19.2

2.2. Crystallization

Initial crystallization screens were set up with a Honeybee crystallization robot (Genomic Solutions) using both in-house and commercial crystallization screens (Hampton Research, DeCode Genetics). Crystals grew in several conditions of the commercial screens, but were too small to be used without optimization. Using our locally developed screen, bipyramidal crystals (0.075 × 0.05 × 0.02 mm) were grown in 2–4 h using the sitting-drop vapor-diffusion method at 295 K from drops containing 200 nl protein solution (10 mg ml^{-1} in 50 m*M* Tris pH 8.0, 100 m*M* sodium chloride, 5 m*M* DTT), 200 nl water and 200 nl reservoir solution (20% MPD, 0.1 *M* sodium cacodylate pH 6.0). Larger crystals with typical dimensions of 0.30 × 0.20 × 0.075 mm were obtained in hanging drops by increasing reagent volumes to 1 µl protein sample, 2 µl water and 2 µl reservoir solution (Fig. 1). The MPD present in the crystallization condition was sufficient for successful flash-cooling and thus no further cryoprotectants were added. Crystals were mounted in cryoloops (Hampton Research) and flash-cooled by direct immersion into liquid nitrogen prior to X-ray diffraction analysis.

2.3. Data collection and processing

X-ray diffraction data were collected on beamline 8.3.1 at the Advanced Light Source (Berkeley). The presence of two or more lattices in the diffraction pattern of several crystals indicated a problem with non-merohedral twinning. By using a 30 µm collimator and systematic translation of a crystal using a scripted procedure (J. Holton, unpublished results) we could find a region near the edge of a crystal that was not twinned. Two data sets of 180 images each (1 s and 10 s exposures) were collected on an ADSC Quantum 210 CCD detector with a crystal-to-detector distance of 150 mm. Intensity data were collected at 100 K using a wavelength of 1.1 Å and a 0.5° oscillation angle per image was chosen based on the relatively low mosaicity of ∼0.3°. Diffraction data were integrated with *MOSFLM* (Leslie, 1992), followed by scaling and merging with *SCALA* from the *CCP*4 suite of programs (Collaborative Computational Project, Number 4, 1994). Diffraction data statistics are

summarized in Table 1. Based on systematic absences, the space group was assigned as $C222_1$, with unit-cell parameters a = 61.98, b = 67.57, c = 108.55 Å, $\alpha = \beta = \gamma = 90^\circ$. Analysis of the self-rotation function revealed a significant non-origin peak at 5.1σ above the background, indicating that there are two EVM053 monomers per asymmetric unit. This gives a Matthews volume of 2.2 Å^3 Da^{-1} (Matthews, 1968) and an estimated solvent content of 42.6% within the asymmetric unit. The NCS operation is a 90° rotation around the c axis, resulting in a pseudo-tetrameric space group. However, imposing a tetrameric space group during integration failed, as a γ angle of 90° was incompatible with the observed lattice. The pseudo-symmetry may have contributed to the formation of non-merohedral twinning. Structure solution of EVM053 *via* molecular replacement is currently being undertaken using the PLTT crystal structure (PDB code 1kte; Katti *et al.*, 1995) as the search model.

We thank L. Price for assistance in crystallization and Dr J. Holton for assistance at beamline 8.3.1. Ectromelia DNA was kindly provided by Dr M. Barry. This work is supported by an operating grant from PENCE. X-ray diffraction data was collected at beamline 8.3.1 at the Advanced Light Source (ALS) at Lawrence Berkeley Laboratory under an agreement with the Alberta Synchrotron Institute (ASI). The ALS is operated by the Department of Energy and supported by the National Institutes of Health. Beamline 8.3.1 was funded by the National Science Foundation, the University of California and Henry Wheeler. The ASI synchrotron-access program is supported by grants from the Alberta Science and Research Authority (ASRA) and the Alberta Heritage Foundation for Medical Research (AHFMR).

References

Berardi, M. J., Pendred, C. L. & Bushweller, J. H. (1998). *Biochemistry*, **37**, 5849–5857.
Chai, Y. C., Hoppe, G. & Sears, J. (2003). *Exp. Eye Res.* **76**, 155–159.
Collaborative Computational Project, Number 4 (1994). *Acta Cryst.* D**50**, 760–763.
Fernandes, A. P. & Holmgren, A. (2004). *Antioxid. Redox. Signal.* **6**, 63–74.
Gravina, S. A. & Mieyal, J. J. (1993). *Biochemistry*, **32**, 3368–3376.
Holmgren, A. (1976). *Proc. Natl Acad. Sci. USA*, **73**, 2275–2279.
Katti, S. K., Robbins, A. H., Yang, Y. & Wells, W. W. (1995). *Protein Sci.* **4**, 1998–2005.
Leslie, A. G. W. (1992). *Jnt CCP4–ESF/EACBM Newsl. Protein Crystallogr.* **26**.
Luthman, M., Eriksson, S., Holmgren, A. & Thelander, L. (1979). *Proc. Natl Acad. Sci. USA*, **76**, 2158–2162.
Matthews, B. W. (1968). *J. Mol. Biol.* **33**, 491–497.
Rajagopal, I., Ahn, B. Y., Moss, B. & Mathews, C. K. (1995). *J. Biol. Chem.* **270**, 27415–27418.
Sun, C., Berardi, M. J. & Bushweller, J. H. (1998). *J. Mol. Biol.* **280**, 687–701.